



OPEN ACCESS

EDITED BY
Yonghui Li,
The University of Sydney, Australia

REVIEWED BY
Deshuang Zhao,
University of Electronic Science and
Technology of China, China

*CORRESPONDENCE
Yuli Yang,
yyang@lincoln.ac.uk

SPECIALTY SECTION
This article was submitted to Signal
Processing for Communications,
a section of the journal
Frontiers in Signal Processing

RECEIVED 09 June 2022
ACCEPTED 30 June 2022
PUBLISHED 16 August 2022

CITATION
Zheng D and Yang Y (2022), Pseudo-
doppler aided cancellation of self-
interference in full-
duplex communications.
Front. Sig. Proc. 2:965551.
doi: 10.3389/frsip.2022.965551

COPYRIGHT
© 2022 Zheng and Yang. This is an
open-access article distributed under
the terms of the [Creative Commons
Attribution License \(CC BY\)](https://creativecommons.org/licenses/by/4.0/). The use,
distribution or reproduction in other
forums is permitted, provided the
original author(s) and the copyright
owner(s) are credited and that the
original publication in this journal is
cited, in accordance with accepted
academic practice. No use, distribution
or reproduction is permitted which does
not comply with these terms.

Pseudo-doppler aided cancellation of self-interference in full-duplex communications

Dongsheng Zheng¹ and Yuli Yang^{2*}

¹School of Electronics, Peking University, Beijing, China, ²School of Engineering, University of Lincoln, Lincoln, United Kingdom

In this work, a novel scheme is proposed to enhance the self-interference (SI) cancellation in full-duplex communications. Beyond conventional SI cancellation schemes that rely on the SI suppression, our proposed scheme exploits periodic antenna switching to generate the pseudo-Doppler effect, thus completely removing the SI at the fundamental frequency. In this way, the desired signal is readily obtained through a low-pass filter. For the purpose of performance evaluation, the SI cancellation capability is defined as the difference between the output signal-to-interference-plus-noise ratio (SINR) and the input SINR. Theoretical formulations and numerical results validate that our pseudo-Doppler aided scheme has higher SI cancellation capability than the conventional SI suppression schemes. Moreover, the impact of the SI suppression achieved by conventional schemes and the influence of antenna switching timing difference on the practical implementation of the proposed scheme are investigated, to further substantiate the validity of our pseudo-Doppler aided SI cancellation.

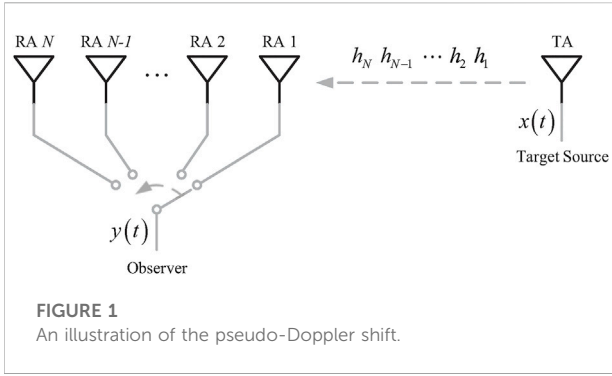
KEYWORDS

pseudo-doppler effect, self-interference cancellation, full-duplex communications, signal-to-interference-plus-noise ratio, timing sequence analysis

1 Introduction

In wireless communications, the Doppler spread, resulting from a relative motion between a pair of transmitter and receiver, is deemed to be a destructive component if the relative motion is very fast, as it is likely to cause frequency dispersion and inter-carrier interference, which will result in poor communication performance (Wang et al., 2006). However, the pseudo-Doppler effect, generated through a change in the wavelength or frequency of a signal received at the observer who is in pseudo motion relative to the signal source, has been favourably exploited by radar and ultrasonic systems in the applications of direction finding, navigation, velocity measurement and vibration assessment (Won et al., 2019).

Motivated by this, we propose a pseudo-Doppler aided scheme to cancel the self-interference (SI) in full-duplex (FD) communications. Although the FD mode has been promoted as an attractive solution to double the spectral efficiency of wireless communications, the inherent SI at FD transceivers imposes a performance bottleneck for the FD operation (Tian et al., 2017; Ma et al., 2020). In the literature, many attempts have been made to remove the obstacle imposed by the strong SI, where



various analog and digital techniques have been developed. In (Zhang et al., 2019), the SI was suppressed by 83 dB, including 45 dB from antenna isolation and 38 dB from adaptive multi-tap analog cancellation. In (Chung et al., 2015), the SI was suppressed by 103 dB, where the antenna isolation, analog and digital cancellations contributed 42 dB, 18 and 43 dB, respectively. In (Anttila et al., 2021), a real-time digital cancellation of 46 dB contributed towards a SI suppression of 103 dB.

The majority of conventional SI cancellation schemes rely on the SI suppression at the receiver (Sabharwal et al., 2014; Kolodziej et al., 2019). To the best of our knowledge, none of the SI cancellation schemes that have been reported can completely remove all the SI from the desired signal. In this work, we exploit the pseudo-Doppler effect to induce controllable frequency shift and completely remove the SI from the desired signal at the fundamental frequency.

The novelty and contribution of this work are three-fold.

- *Approach:* A novel SI cancellation scheme is proposed on the basis of pseudo-Doppler effect.
- *Evaluation:* The SI cancellation capability of the proposed scheme is formulated and compared with that of conventional schemes.
- *Application:* The conditions that the proposed scheme is preferred to conventional ones are investigated.

In the following, the pseudo-Doppler aided SI cancellation scheme is proposed based on the principle of pseudo-Doppler shift. Subsequently, its SI cancellation capability is theoretically analysed and compared with conventional SI cancellation schemes.

2 Motivation: pseudo-doppler shift

The pseudo-Doppler shift originated in radio systems for the purpose of direction finding (Earp and Godfrey, 1947). To cause a pseudo-Doppler shift, a rapid switching between the receive antennas (RAs) of an observer is utilised to imitate the relative

motion between the transmit antenna (TA) of a target source and the observer. As shown in Figure 1, the observer's N RAs are switched sequentially and circularly to receive the signals transmitted from the target source. As long as the switching is sufficiently fast, the target source's direction will be found through the pseudo-Doppler effect caused by the switching. We remark that, the generation of pseudo-Doppler effect does not rely on an actual relative motion between the observer and the target source. For example, given that the distance between two adjacent RAs of the observer is d and the switching between them takes time τ , the switching cycle from RA 1 to RA N is equivalent to the target source moving towards the observer at a velocity of d/τ , while the switching cycle from RA N to RA 1 is equivalent to the target source moving away from the observer at d/τ .

Given that the flat-fading channel coefficients spanning from the TA to the RAs are independent of each other, the observer's received signal, denoted by $y(t)$, is expressed as

$$y(t) = h(t)x(t) + \omega(t), \tag{1}$$

where $h(t)$ is the channel response and $x(t)$ denotes the target source's transmitted signal. The additive white Gaussian noise (AWGN) process $\omega(t)$ has a power spectrum density N_0 .

At the observer, the duration of a whole switching cycle from RA 1 to RA N is T_s and, thus, the identical switching interval of each RA is $\tau = T_s/N$. As such, the channel response $h(t)$ is formulated by a periodic function with period T_s as

$$h(t) = h_n, \quad kT_s + (n-1)\tau \leq t < kT_s + n\tau, \tag{2}$$

$$n = 1, 2, \dots, N,$$

where $k \in \mathbb{Z}$, and h_n is the channel coefficient from the TA to RA n . The Fourier series of $h(t)$ is calculated using the following coefficients:

$$c_0 = \frac{1}{T_s} \int_0^{T_s} h(t) dt = \frac{1}{N} \sum_{n=1}^N h_n, \tag{3}$$

$$c_l = \frac{1}{T_s} \int_0^{T_s} h(t) \exp\left(-j \frac{2\pi l}{T_s} t\right) dt$$

$$= \sum_{n=1}^N \frac{h_n}{T_s} \int_{(n-1)\frac{T_s}{N}}^{n\frac{T_s}{N}} \exp\left(-j \frac{2\pi l}{T_s} t\right) dt \tag{4}$$

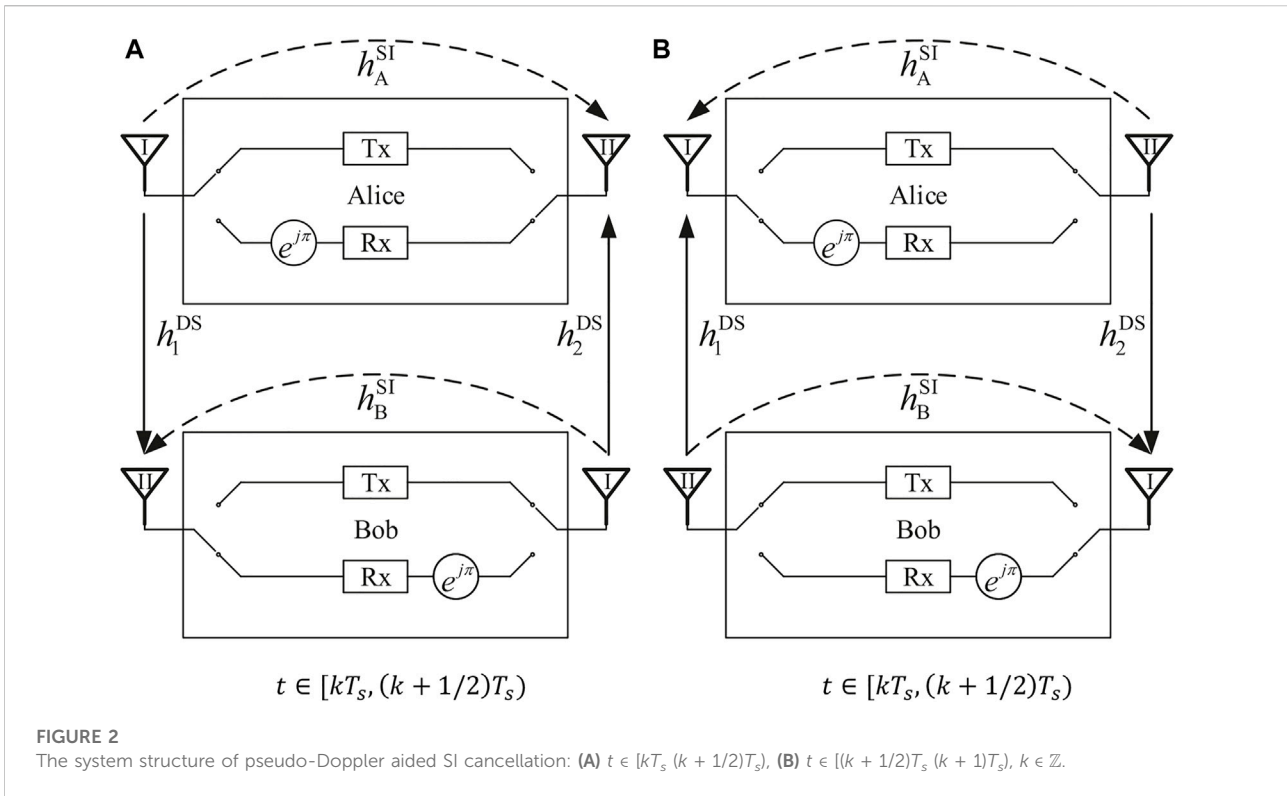
$$= \sum_{n=1}^N \frac{h_n}{j2\pi l} \exp\left(-j \frac{2\pi n l}{N}\right) \left[\exp\left(j \frac{2\pi l}{N}\right) - 1 \right], \quad l \neq 0.$$

As revealed by (4), the l^{th} harmonic has frequency dispersion triggered by the switching between N RAs, $l \neq 0$.

Further, the Fourier transform of the observer's received signal $y(t)$ is obtained by

$$Y(f) = H(f) * X(f) + \Omega(f) = \sum_{l=-\infty}^{+\infty} c_l X(f - lf_s) + \Omega(f), \tag{5}$$

where $*$ is the convolution operator. The Fourier transforms of the channel response $h(t)$ and the AWGN $\omega(t)$ are $H(f) = \sum_{l=-\infty}^{+\infty} c_l \delta(f - lf_s)$ and $\Omega(f)$, respectively. It is obvious that the source's signal $X(f)$ experiences the pseudo-Doppler shift lf_s , $l \neq 0$,



with $f_s = 1/T_s$, denoting the unit pseudo-Doppler shift triggered by the RA switching of cycle duration T_s .

In essence, the pseudo-Doppler shift is induced by the periodic variation of channel coefficients between a pair of transmitter and receiver. Therefore, a periodic antenna switching at the transmitter or at both the transmitter and the receiver can also trigger the same frequency shift as that obtained in (5). Motivated by this, we propose a novel SI cancellation scheme to enhance the FD communication performance, by the aid of a pseudo-Doppler shift, in next Section.

3 Pseudo-doppler aided SI cancellation

For the receiver to retrieve the desired signal in a FD transmission, the majority of conventional SI cancellation schemes, e.g., Zhang et al. (2019); Chung et al. (2015); Anttila et al. (2021), rely on the SI suppression, where the SI is firstly reconstructed and then subtracted from the received signal. Different from this design, we will exploit the pseudo-Doppler effect to completely remove the SI from the desired signal at the fundamental frequency.

Consider the communications between a pair of FD transceivers, Alice and Bob, as shown in Figure 2, where both Alice and Bob periodically switch their antennas to generate the pseudo-Doppler effect. A switching cycle of duration T_s is

divided into two intervals: In the first half cycle, i.e., $t \in [kT_s, (k + 1/2)T_s)$, Antennas I and II of a transceiver is used as its TA and RA, respectively; in the second half cycle, i.e., $t \in [(k + 1/2)T_s, (k + 1)T_s)$, Antennas I and II of a transceiver is used as its RA and TA, respectively, $k \in \mathbb{Z}$. In addition, the received signal phase is shifted by π in the second half cycle, for the generation of a SI signal opposite to the SI in the first half cycle. Thanks to the symmetric system structure, the received signals of Alice and Bob can be expressed in the same form as

$$y(t) = h_{DS}(t)x_{DS}(t) + h_{SI}(t)x_{SI}(t) + \omega(t), \quad (6)$$

where $h_{DS}(t)$ and $h_{SI}(t)$ are the channel responses to the desired signal, denoted by $x_{DS}(t)$, and the SI, denoted by $x_{SI}(t)$, respectively.

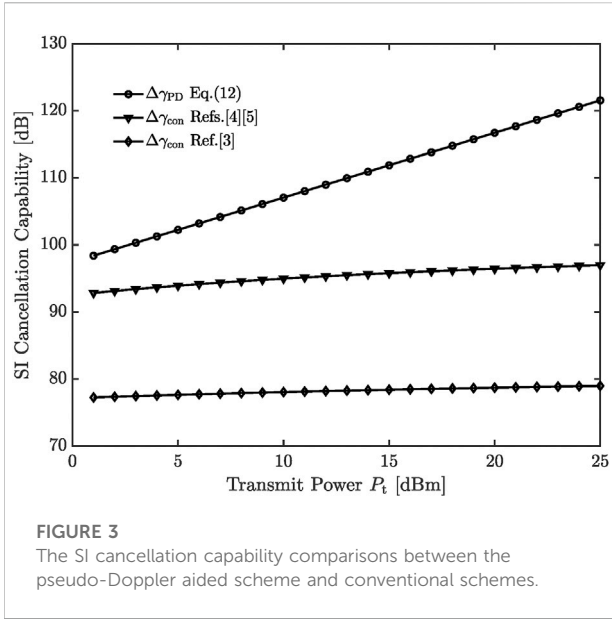
Next, we will focus on the SI cancellation at Bob, as the SI cancellation at Alice can be analysed in the same way. As regards the periodic antenna switching at both Alice and Bob, Bob's channel responses to his desired signal and SI can be written as

$$h_{DS}(t) = \begin{cases} h_1^{DS}, & kT_s \leq t < (k + 1/2)T_s, \\ -h_2^{DS}, & (k + 1/2)T_s \leq t < (k + 1)T_s, \end{cases} \quad (7)$$

and

$$h_{SI}(t) = \begin{cases} h_B^{SI}, & kT_s \leq t < (k + 1/2)T_s, \\ -h_B^{SI}, & (k + 1/2)T_s \leq t < (k + 1)T_s, \end{cases} \quad (8)$$

respectively, where h_1^{DS} is the channel coefficient between Alice's Antenna I and Bob's Antenna II, and h_2^{DS} is the



channel coefficient between Alice’s Antenna II and Bob’s Antenna I. Moreover, h_B^{SI} is Bob’s SI channel coefficient, i.e., between his own Antennas I and II. Specifically, the SI channel responses in the first and second half cycles are opposite to each other, because of a phase shift π introduced in the reciprocal channel.

Referring to (3) and (4), we have the coefficients for the Fourier series of $h_{DS}(t)$ as

$$c_0^{DS} = \frac{h_1^{DS} - h_2^{DS}}{2}, c_l^{DS} = \begin{cases} \frac{h_1^{DS} + h_2^{DS}}{j\pi l}, & l \text{ is odd;} \\ 0, & l \text{ is even and } l \neq 0. \end{cases} \quad (9)$$

Similarly, the coefficients for the Fourier series of $h_{SI}(t)$ are

$$c_0^{SI} = \frac{h_B^{SI} - h_B^{SI}}{2} = 0, c_l^{SI} = \begin{cases} \frac{2h_B^{SI}}{j\pi l}, & l \text{ is odd;} \\ 0, & l \text{ is even and } l \neq 0. \end{cases} \quad (10)$$

As such, the SI channel response at the fundamental frequency, c_0^{SI} , is nullified. In addition, the channel responses to both the desired signal and the SI are nullified at the frequency lf_s with $l \in \{\pm 2, \pm 4, \dots\}$. Such a frequency is called *interference-free frequency*, which can be used to accommodate another FD communication link within the same cellular resource for avoiding intra-cell interference. The frequencies lf_s with $l = \pm 1, \pm 3, \dots$ are *interference frequencies* to serve in other cells for improving the whole cellular network throughput.

Then, referring to (5), we obtain the frequency-domain expression of Bob’s received signal $y(f)$ given in (6) as

$$\begin{aligned} Y(f) &= H_{DS}(f) * X_{DS}(f) + H_{SI}(f) * X_{SI}(f) + \Omega(f) \\ &= \frac{h_1^{DS} - h_2^{DS}}{2} X_{DS}(f) + \sum_{l=2k-1} \frac{h_1^{DS} + h_2^{DS}}{j\pi l} X_{DS}(f - lf_s) \\ &\quad + \sum_{l=2k-1} \frac{2h_B^{SI}}{j\pi l} X_{SI}(f - lf_s) + \Omega(f), \quad k \in \mathbb{Z} \end{aligned} \quad (11)$$

where $X_{DS}(f)$ and $X_{SI}(f)$ denote the Fourier transforms of the desired signal $x_{DS}(t)$ and the SI $x_{SI}(t)$, respectively.

As shown in (11), the SI has been completely removed from the received signal at the fundamental frequency and, therefore, we may readily obtain the desired signal using a low-pass filter at the fundamental frequency. To guarantee that the desired signal is perfectly filtered from the received signal, the antenna switching cycle duration T_s should be set to $T_s \leq 1/(2B)$, i.e., the unit pseudo-Doppler shift $f_s \geq 2B$, where B is the bandwidth of the desired signal.

It is noted that the channel reciprocity is of critical importance to a complete removal of the SI at the fundamental frequency. Herein, we further validate the assumption of channel reciprocity over the SI path(s). In general, there are three types of SI-coupling path(s): the line-of-sight (LoS) path, the fixed-reflection paths, and the moving-reflection paths (Kolodziej et al., 2019). For the LoS path and the fixed-reflection paths, accurate calibration of the transceiver radio frequency chains guarantees the channel reciprocity. For the moving-reflection paths, the channel reciprocity can also be achieved within the coherence time. In practice, the efficacy of our pseudo-Doppler aided SI cancellation can be guaranteed within current frame-based wireless systems, where the frame length is determined by the coherence time.

4 Performance evaluation

In this section, the SI cancellation capability of our pseudo-Doppler aided scheme is investigated and compared with that of conventional SI cancellation schemes, based on which the conditions that our scheme is preferred to conventional ones are quantified in terms of outage probability. Herein, the block fading channel model is adopted, where the channel coefficients remain constant within a coherence time and change to an independent status in the next coherence time. This process is repeated for each coherent time and, therefore, the coherence time (i.e., the velocity of a moving terminal) is not an explicit factor in the channel model.

4.1 SI cancellation capability

The SI cancellation capability of the proposed pseudo-Doppler aided scheme is defined in dB as

$$\Delta\gamma_{PD} = \log_{10} \bar{\gamma}_{PD} - \log_{10} \bar{\gamma}_{in}, \quad (12)$$

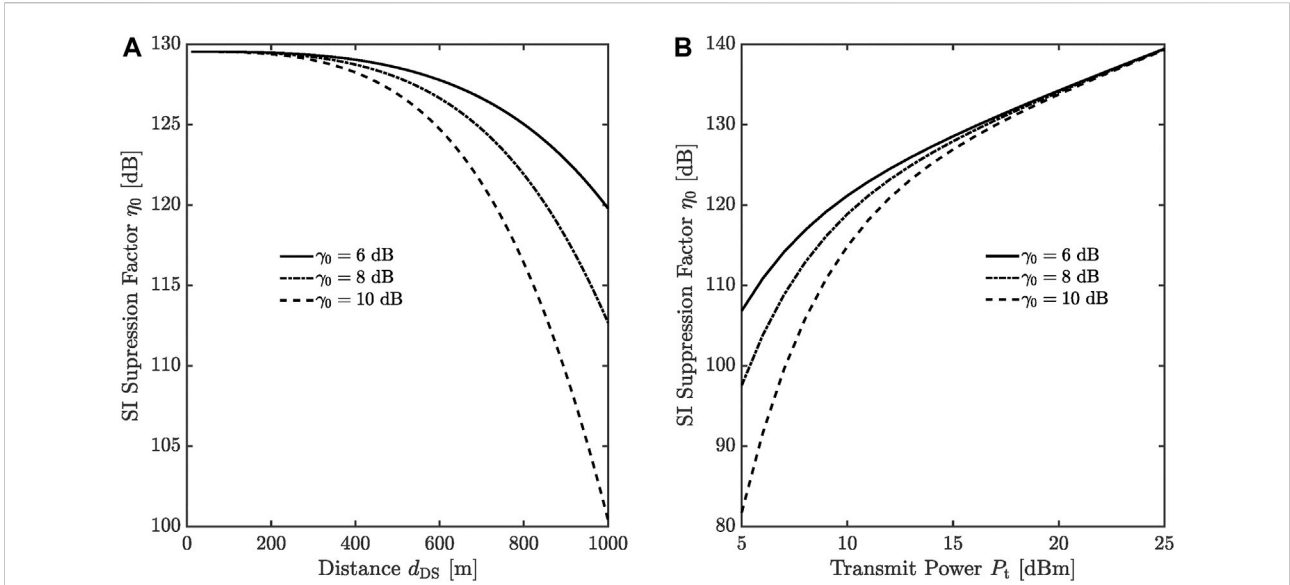


FIGURE 4 The SI suppression factor η_0 : (A) versus the distance d_{DS} , (B) versus the transmit power P_t .

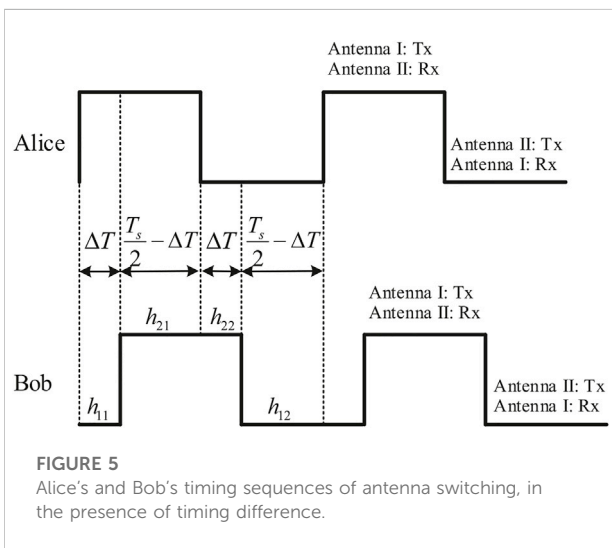


FIGURE 5 Alice's and Bob's timing sequences of antenna switching, in the presence of timing difference.

where $\bar{\gamma}_{PD} = \mathcal{E}\{\gamma_{PD}\}$ is the mean output signal-to-interference-plus-noise ratio (SINR) of our pseudo-Doppler aided SI cancellation, and $\bar{\gamma}_{in} = \mathcal{E}\{\gamma_{in}\}$ is the mean SINR in the case that there is no SI cancellation applied, i.e., equal to the mean input SINR of conventional SI cancellation schemes.

As shown in (11), the desired signal can be filtered free of the SI at the fundamental frequency $l = 0$. Hence, the output SINR γ_{PD} is formulated as

$$\gamma_{PD} = \frac{P_t |c_0^{DS}|^2}{BN_0} = \frac{P_t |h_1^{DS} - h_2^{DS}|^2}{4BN_0}, \quad (13)$$

where P_t is the transmit power. Herein, the channel coefficients h_1^{DS} and h_2^{DS} are further modelled as

$$h_1^{DS} = \sqrt{G} d_{DS}^{-\phi/2} g_1^{DS} \quad (14)$$

and

$$h_2^{DS} = \sqrt{G} d_{DS}^{-\phi/2} g_2^{DS}, \quad (15)$$

where G and ϕ are the path-loss constant and exponent, respectively. The distance between Alice and Bob is d_{DS} . Moreover, the small-scale fading g_1^{DS} and g_2^{DS} follow a complex Gaussian distribution with zero mean and unit variance, $\mathcal{CN}(0, 1)$.

Substituting (14) and (15) into (13), we have

$$\gamma_{PD} = \frac{P_t G d_{DS}^{-\phi} |g_1^{DS} - g_2^{DS}|^2}{4BN_0}, \quad (16)$$

which follows an exponential distribution with mean

$$\bar{\gamma}_{PD} = \frac{P_t G d_{DS}^{-\phi}}{2BN_0} \triangleq \bar{\gamma}_{DS} / 2. \quad (17)$$

Thus, the probability density function (pdf) of γ_{PD} is

$$f_{\gamma_{PD}}(\gamma) = \begin{cases} (2/\bar{\gamma}_{DS}) \exp(-2\gamma/\bar{\gamma}_{DS}), & \gamma \geq 0; \\ 0, & \gamma < 0. \end{cases} \quad (18)$$

The SINR without any SI cancellation, γ_{in} , is expressed as

$$\gamma_{in} = \frac{P_t G d_{DS}^{-\phi} |g_1^{DS}|^2}{P_t G d_{SI}^{-\phi} |g_B^{SI}|^2 + BN_0} = \frac{\bar{\gamma}_{DS} |g_1^{DS}|^2}{\bar{\gamma}_{SI} |g_B^{SI}|^2 + 1}, \quad (19)$$

where $\bar{\gamma}_{SI} = P_t G d_{SI}^{-\phi} / (BN_0)$ is the mean SI to noise power ratio, with d_{SI} denoting the distance between Bob's Antennas I and II. The small-scale fading $g_B^{SI} \sim \mathcal{CN}(0, 1)$.

Based on (Kwon et al., 2010, Eq. 5), the cumulative distribution function (cdf) of γ_{in} is obtained by

$$F_{\gamma_{in}}(\gamma) = \begin{cases} 1 - \frac{1}{1 + (\bar{\gamma}_{SI}/\bar{\gamma}_{DS})\gamma} \exp\left(-\frac{\gamma}{\bar{\gamma}_{DS}}\right), & \gamma \geq 0; \\ 0, & \gamma < 0. \end{cases} \quad (20)$$

Then, the mean SINR without any SI cancellation is

$$\bar{\gamma}_{in} = \int_0^{\infty} \gamma dF_{\gamma_{in}}(\gamma) = \frac{\bar{\gamma}_{DS}}{\bar{\gamma}_{SI}} \exp\left(\frac{1}{\bar{\gamma}_{SI}}\right) \left[-\text{Ei}\left(-\frac{1}{\bar{\gamma}_{SI}}\right)\right], \quad (21)$$

where $\text{Ei}(x) = -\int_{-x}^{+\infty} (e^{-t}/t)dt$ is the exponential integral.

As a result, the SI cancellation capability of our pseudo-Doppler aided scheme is obtained by substituting (17) and (21) into (12), which is compared with the SI cancellation capability of conventional schemes in Figure 3. The conventional SI cancellation capability is expressed in dB as

$$\Delta\gamma_{con} = \log_{10} \bar{\gamma}_{con} - \log_{10} \bar{\gamma}_{in}, \quad (22)$$

where $\bar{\gamma}_{con} = \varepsilon\{\gamma_{con}\}$ is the mean output SINR of conventional SI cancellation schemes, and the output SINR

$$\gamma_{con} = \frac{\bar{\gamma}_{DS} |g_1^{DS}|^2}{\bar{\gamma}_{SI} |g_B^{SI}|^2 / \eta + 1} \quad (23)$$

with η for the SI suppression factor. More specifically, the mean residual SI to noise power ratio is $\bar{\gamma}_{res} = \bar{\gamma}_{SI}/\eta$. Referring to the derivation of (21), we obtain the mean output SINR of conventional SI cancellation schemes as

$$\bar{\gamma}_{con} = \frac{\bar{\gamma}_{DS}}{\bar{\gamma}_{res}} \exp\left(\frac{1}{\bar{\gamma}_{res}}\right) \left[-\text{Ei}\left(-\frac{1}{\bar{\gamma}_{res}}\right)\right]. \quad (24)$$

In Figure 3, the distance between Alice and Bob, $d_{DS} = 100$ m. The distance between Antennas I and II, $d_{SI} = 0.05$ m. The path-loss constant $G = -31.5$ dB, and the path-Loss exponent $\phi = 3$. The AWGN power spectral density $N_0 = -174$ dBm/Hz, and the bandwidth $B = 5$ MHz. As shown in this figure, our pseudo-Doppler aided scheme has a much stronger capability in the SI cancellation than the conventional schemes that rely on the SI suppression.

4.2 Impact of SI suppression factor

With the rapid development of signal processing technologies, a growth is anticipated in the SI suppression

factor of conventional schemes. Herein, the impact of the SI suppression factor on the application of our pseudo-Doppler aided scheme is investigated in terms of the output SINR outage probability.

The outage probability of output SINR is defined as the probability that the output SINR falls below a predetermined threshold γ_0 . Hence, the outage probability of the output SINR γ_{PD} in our pseudo-Doppler aided scheme is

$$\Pr(\gamma_{PD} \leq \gamma_0) = \int_0^{\gamma_0} f_{\gamma_{PD}}(\gamma) d\gamma = 1 - \exp\left(-\frac{2\gamma_0}{\bar{\gamma}_{DS}}\right), \quad (25)$$

where the pdf $f_{\gamma_{PD}}(\gamma)$ is given in (18). The outage probability of the output SINR γ_{con} in conventional schemes is

$$\Pr(\gamma_{con} \leq \gamma_0) = F_{\gamma_{con}}(\gamma_0) = 1 - \frac{1}{1 + (\bar{\gamma}_{res}/\bar{\gamma}_{DS})\gamma_0} \exp\left(-\frac{\gamma_0}{\bar{\gamma}_{DS}}\right), \quad (26)$$

where the cdf of γ_{con} , $F_{\gamma_{con}}(\gamma)$, is obtained from (20) by replacing $\bar{\gamma}_{SI}$ with $\bar{\gamma}_{res} = \bar{\gamma}_{SI}/\eta$.

Given the threshold γ_0 , our pseudo-Doppler aided scheme is preferred to conventional ones in the condition that $\Pr(\gamma_{PD} \leq \gamma_0) < \Pr(\gamma_{con} \leq \gamma_0)$, where we have

$$\eta < \gamma_0 \left(\frac{d_{DS}}{d_{SI}}\right)^\phi \left[\exp\left(\frac{\gamma_0 N_0 B d_{DS}^\phi}{P_t G}\right) - 1\right]^{-1} \triangleq \eta_0. \quad (27)$$

In other words, our pseudo-Doppler aided scheme outperforms conventional ones when their SI suppression factor is lower than η_0 defined in (27). The SI suppression factor η_0 is plotted versus the distance between Alice and Bob, d_{DS} , in Figure 4A, where the transmit power $P_t = 15$ dBm. Meanwhile, η_0 is plotted versus the transmit power P_t in Figure 4B, where the distance $d_{DS} = 500$ m. The other simulation parameters are set the same as those in Figure 3.

As shown in these figures, η_0 decreases as the threshold γ_0 or the distance d_{DS} increases, which implies that conventional schemes need lower SI suppression factors to compete with the SI cancellation capability of the proposed scheme if there is a higher requirement on the output SINR or a larger distance between Alice and Bob. However, the SI suppression factors in Figure 4 are still too high for the SI cancellation schemes that have been reported to achieve.

In addition, η_0 increases as the transmit power P_t increases, which can be derived from the definition of η_0 in (27) as well. The main reason behind this is that our pseudo-Doppler aided scheme completely removes the SI from the desired signal at the fundamental frequency, while the residual SI in conventional cancellation schemes increases with the increase in the transmit power P_t .

4.3 Impact of antenna switching timing difference

From the design presented in Section 3, we may find that Alice and Bob need to synchronise their antenna switching timing in the pseudo-Doppler aided SI cancellation. However, due to sync error, there might be a timing difference between them in practice. Given that both Alice’s and Bob’s antenna switching cycles are T_s , the timing difference, denoted by ΔT , is illustrated in Figure 5, where h_{ba} is the channel coefficient from Alice’s Antenna a to Bob’s Antenna b , $a, b \in \{1, 2\}$. In this regard, Bob’s channel response to Alice’s signal is formulated as.

$$h_{DS}^{\Delta T}(t) = \begin{cases} h_{21}, & kT_s \leq t < (k + 1/2)T_s - \Delta T, \\ h_{22}, & (k + 1/2)T_s - \Delta T \leq t < (k + 1/2)T_s, \\ -h_{12}, & (k + 1/2)T_s \leq t < (k + 1)T_s - \Delta T, \\ -h_{11}, & (k + 1/2)T_s - \Delta T \leq t < (k + 1)T_s, \end{cases} \quad (28)$$

The Fourier series of $h_{DS}^{\Delta T}(t)$ is calculated using.

$$c_0^{\Delta T} = \frac{1}{T_s} \int_0^{T_s} h_{DS}^{\Delta T}(t) dt = \frac{h_{21} - h_{12}}{2} + \frac{\Delta T(h_{22} + h_{12} - h_{21} - h_{11})}{T_s}, \quad (29)$$

$$c_l^{\Delta T} = \frac{1}{T_s} \int_0^{T_s} h_{DS}^{\Delta T}(t) \exp\left(-j \frac{2\pi l}{T_s} t\right) dt = \begin{cases} \frac{h_{12} + h_{21}}{j2\pi l} (1 + \alpha) - \frac{h_{11} + h_{22}}{j2\pi l} (1 - \alpha), & l \text{ is odd,} \\ \frac{h_{22} + h_{12} - h_{21} - h_{11}}{j2\pi l} (1 - \alpha), & l \text{ is even and } l \neq 0, \end{cases} \quad (30)$$

Where $\alpha = \exp(-j2\pi l \Delta T / T_s)$ is used for ease of notation.

On the other hand, Bob’s channel response to the SI in the presence of timing difference is the same as that without timing difference, i.e., given by (8), which indicates that the timing difference has no influence on the SI removal at the fundamental frequency $l = 0$.

Thus, the mean SINR at the output of the low-pass filter can be derived as

$$\bar{\gamma}_{PD}^{\Delta T} = \varepsilon \left\{ \frac{P_t |c_0^{\Delta T}|^2}{BN_0} \right\} = \frac{16(\Delta T - T_s/4)^2 + T_s^2}{4T_s^2} \bar{\gamma}_{DS}. \quad (31)$$

Obviously, the mean SINR $\bar{\gamma}_{PD}^{\Delta T}$ achieves its maximum value $\bar{\gamma}_{DS}/2$ at $\Delta T = 0, T_s/2$ and its minimum value $\bar{\gamma}_{DS}/4$ at $\Delta T = T_s/4$. In comparison with (17), the maximum performance loss caused by the timing difference is 3 dB only.

References

Anttila, L., Lampu, V., Hassani, S., Campo, P., Korpi, D., Turunen, M., et al. (2021). Full-duplexing with sdr devices: Algorithms, fpga implementation, and real-time results. *IEEE Trans. Wirel. Commun.* 20, 2205–2220. doi:10.1109/TWC.2020.3040226

5 Discussion

In this work, a novel SI cancellation scheme, referred to as pseudo-Doppler aided cancellation, was proposed for FD communications to completely remove the SI from the desired signal and leave null residual SI at the fundamental frequency. In comparison to the conventional SI cancellation schemes that rely on the SI suppression, illustrative numerical results substantiated that the proposed scheme achieved much better performance in terms of SI cancellation capability.

Concerning the mixing of the desired signal and the SI at the pseudo-Doppler shifted frequencies, the development of advanced SI suppression technologies and the integration of our pseudo-Doppler aided SI cancellation with them are to be pursued for getting higher desired signal power at the receiver, aiming to further improve the output SINR.

Data availability statement

The raw data supporting the conclusions of this article will be made available by the authors, without undue reservation.

Author contributions

DZ and YY contributed to conception and design of the study. DZ performed the statistical analysis and wrote the first draft of the manuscript. YY revised the draft and approved the submitted version.

Conflict of interest

The authors declare that the research was conducted in the absence of any commercial or financial relationships that could be construed as a potential conflict of interest.

Publisher’s note

All claims expressed in this article are solely those of the authors and do not necessarily represent those of their affiliated organizations, or those of the publisher, the editors and the reviewers. Any product that may be evaluated in this article, or claim that may be made by its manufacturer, is not guaranteed or endorsed by the publisher.

Chung, M., Sim, M., Kim, J., Kim, D., and Chae, C. (2015). Prototyping real-time full duplex radios. *IEEE Commun. Mag.* 53, 56–63. doi:10.1109/MCOM.2015.7263346

- Earp, C., and Godfrey, R. (1947). Radio direction-finding by the cyclical differential measurement of phase. *J. Institution Electr. Eng.* 94, 705–721. doi:10.1049/ji-3a-2.1947.0091
- Kolodziej, K., Perry, B., and Herd, J. (2019). In-band full-duplex technology: Techniques and systems survey. *IEEE Trans. Microw. Theory Tech.* 67, 3025–3041. doi:10.1109/TMTT.2019.2896561
- Kwon, T., Lim, S., Choi, S., and Hong, D. (2010). Optimal duplex mode for df relay in terms of the outage probability. *IEEE Trans. Veh. Technol.* 59, 3628–3634. doi:10.1109/TVT.2010.2050503
- Ma, M., Tian, S., Chen, Y., Wang, L., Yang, Y., Wan, L., et al. (2020). A prototype of co-frequency co-time full duplex networking. *IEEE Wirel. Commun.* 27, 132–139. doi:10.1109/MWC.001.1800565
- Sabharwal, A., Schniter, P., Guo, D., Bliss, D., Rangarajan, S., Wichman, R., et al. (2014). In-band full-duplex wireless: Challenges and opportunities. *IEEE J. Sel. Areas Commun.* 32, 1637–1652. doi:10.1109/JSAC.2014.2330193
- Tian, S., Ma, M., Yang, Y., and Jiao, B. (2017). Blind analog interference cancellation. *IEEE Commun. Lett.* 21, 1867–1870. doi:10.1109/LCOMM.2017.2694427
- Wang, T., Proakis, J., Masry, E., and Zeidler, J. (2006). Performance degradation of ofdm systems due to Doppler spreading. *IEEE Trans. Wirel. Commun.* 5, 1422–1432. doi:10.1109/TWC.2006.1638663
- Won, H., Isbel, K., Vanderburgh, L., Platt, J., Lee, W., Hong, Y., et al. (2019). Developing a direction-finding system and channel sounder using a pseudo-Doppler antenna array [education corner]. *IEEE Antennas Propag. Mag.* 61, 84–89. doi:10.1109/MAP.2019.2920047
- Zhang, L., Ma, M., and Jiao, B. (2019). Design and implementation of adaptive multi-tap analog interference canceller. *IEEE Trans. Wirel. Commun.* 18, 1698–1706. doi:10.1109/TWC.2019.2895635